Available online at www.sciencedirect.com

ScienceDirect

Advances in Space Research 59 (2017) 503–512

ADVANCES IN SPACE RESEARCH (a COSPAR publication)

www.elsevier.com/locate/asr

Global surface temperature change analysis based on MODIS data in recent twelve years

K.B. Mao [a,b,g,*], Y. Ma [a,g], X.L. Tan [c], X.Y. Shen [d], G. Liu [b], Z.L. Li [a], J.M. Chen [e], L. Xia [f]

[a] National Hulunber Grassland Ecosystem Observation and Research Station, Institute of Agricultural Resources and Regional Planning, Chinese Academy of Agricultural Sciences, Beijing 100081, China

[b] State Key Laboratory of Remote Sensing Science, Institute of Remote Sensing and Digital Earth Research, Chinese Academy of Science and Beijing Normal University, Beijing 100086, China

[c] College of Resources and Environments, Hunan Agricultural University, Changsha 410128, China

[d] Hydrometeorology and Remote Sensing Laboratory, University of Oklahoma, Norman 73072, USA

[e] International Institute for Earth System Science, Nanjing University, Nanjing, China

[f] Beijing Research Center of Intelligent Equipment for Agriculture, Beijing Academy of Agriculture and Forestry Science, Beijing 100097, China

[g] International Agricultural Big Data and Nutrition Academy in China, Hong Kong 999077, China

Received 3 December 2015; received in revised form 25 October 2016; accepted 4 November 2016
Available online 12 November 2016

Abstract

Global surface temperature change is one of the most important aspects in global climate change research. In this study, in order to overcome shortcomings of traditional observation methods in meteorology, a new method is proposed to calculate global mean surface temperature based on remote sensing data. We found that (1) the global mean surface temperature was close to 14.35 °C from 2001 to 2012, and the warmest and coldest surface temperatures of the global in the recent twelve years occurred in 2005 and 2008, respectively; (2) the warmest and coldest surface temperatures on the global land surface occurred in 2005 and 2001, respectively, and on the global ocean surface in 2010 and 2008, respectively; and (3) in recent twelve years, although most regions (especially the Southern Hemisphere) are warming, global warming is yet controversial because it is cooling in the central and eastern regions of Pacific Ocean, northern regions of the Atlantic Ocean, northern regions of China, Mongolia, southern regions of Russia, western regions of Canada and America, the eastern and northern regions of Australia, and the southern tip of Africa. The analysis of daily and seasonal temperature change indicates that the temperature change is mainly caused by the variation of orbit of celestial body. A big data model based on orbit position and gravitational-magmatic change of celestial body with the solar or the galactic system should be built and taken into account for climate and ecosystems change at a large spatial-temporal scale.

Keywords: Surface temperature; Global; Climate change

1. Introduction

Many reports suggest that extreme floods, heat waves, droughts, and wildfires that occurred on a global scale over the past decade might be increased by climate change (Rahmstorf and Coumou, 2011). For instance, the heat wave affecting Australia in the summer of 2013 brought extreme temperatures to most part of the Australian continent over a prolonged period. Climate change was a major driving force behind many extreme weather events that alternately scorched and soaked many countries in recent years. People often guessed "this year is the warmest" or "this year is the coldest". Numerous studies have been

* Corresponding author at: National Hulunber Grassland Ecosystem Observation and Research Station, Institute of Agricultural Resources and Regional Planning, Chinese Academy of Agricultural Sciences, Beijing 100081, China.
E-mail address: maokebiao@126.com (K.B. Mao).

http://dx.doi.org/10.1016/j.asr.2016.11.007
0273-1177/

carried out to quantify the global temperature, which are usually based on data from meteorological stations (Hansen et al., 2010; Brohan et al., 2006; Smith et al., 2008; Ishihara, 2006; Rahmstorf and Coumou, 2011). There are four major global temperature indices that incorporate station data. These efforts are led, respectively, by NOAA's National Climate Data Center (NOAA NCDC), NASA's Goddard Institute of Space Sciences (NASA GISS), a collaboration between the University of East Anglia's Climatic Research Unit, the UK Met Office's Hadley Centre (CRU), and the Berkeley Earth Surface Temperature group. These groups individually utilize different averaging techniques, quality control procedures, homogenization techniques, and datasets, but all primarily rely on the Global Historical Climatology Network (GHCN) for their input data. The GHCN data collects data from about 7000 stations (Hansen et al., 1988, 1999, 2001, 2006; Rayner et al., 2003; Fan and Dool, 2008; Jones et al., 1999). The GISS achieved temperature show some differences. For example, GISS and NCDC indicate 2005 as the warmest year in their analyses, while HadCRUT has 1998 as the warmest year. The differences might be caused by two main factors: (1) the way that temperature anomalies are extrapolated, or not extrapolated, into regions without observing stations and (2) the ocean data sets that are employed different by different studies. The detail analysis can be referred to reference (Hansen et al., 2010).

Most analysis concerns only temperature anomalies, not magnitude temperature. Temperature anomalies are computed relative to the base period 1951–1980 (Hansen et al., 2006, 2012). The reason for the focus on anomalies rather than absolute temperature is because absolute temperature varies markedly in space, while monthly or annual temperature anomalies are representative of a much larger region. It is very difficult to determine the annual mean of absolute temperature because temperature variations are different in different regions. The number of ground observation sites is insufficient, especially in mountainous regions, ocean regions, and the Polar regions. Hansen and Lebedeff have shown that surface air temperature anomalies are strongly correlated to distances of the order of 1000 km (Hansen and Lebedeff, 1987). To compensate for sea temperature observations, the surface temperature from satellite sensors (NOAA/AVHRR) is used as a supplement (Hansen et al., 1999). Additional *in situ* and satellite data improve the accuracy of a blended (*in situ* and satellite) sea-surface temperature (SST) (Brohan et al., 2006; Smith et al., 2008; Reynolds et al., 2005). The surface temperature retrieved from satellites is different from near surface air temperature. The surface brightness temperature is influenced by surface emissivity far more than near surface air temperature. Generally speaking, surface temperature varies from point to point on the ground, and ground measurements are generally point measurements. The location of observation sites therefore, has some influence on the measurements. Hansen et al. (2010) tested alternative choices for the ocean data, and showed how global temperature changes were sensitive to estimated temperature changes in polar region where observations are limited. For some meteorological observations, it is difficult to guarantee consistent data recording and proofreading because meteorological observations are made different in many nations. For a more detailed discussion, we can find more information from the The Elusive Absolute Surface Air Temperature (http://data.giss.nasa.gov/gistemp/abs_temp.html).

The history of surface temperature retrieval from remotely sensed thermal infrared (TIR) data dates back to the 1970s (McMillin, 1975). To improve the estimating surface temperature from satellite thermal data, many studies have been carried out, and different algorithms have been proposed to eliminate the influence of emissivity and atmospheric (Becker and Li, 1990; Gillespie et al., 1998; Hook et al., 1992; Kealy and Hook, 1993; Kerr et al., 1992; Pozo et al., 1997; Price, 1983, 1984; Qin et al., 2001; Susskind et al., 1984; Wan and Dozier, 1996; Jiménez-Muñoz and Sobrino, 2003; Mao et al., 2005, 2007). Li et al. (2013a,b) evaluated the advantage and disadvantage of different algorithms in details. NASA has two polar-orbiting Earth Observing System (EOS) satellites (Terra and Aqua) with one satellite passing the equator in the morning (10:30) and evening (22:30) and the other passing the equator in the afternoon (13:30) and late morning (1:30). The reason to have them is on a sun-synchronous, and near-polar orbit is that they can travel from the North Pole to the South Pole on the sunlit side as the Earth rotates below it. As result, they pass over Earth at approximately the same local time each day to ensure comparable daylight conditions during a day. Moderate Resolution Imaging Spectroradiometer (MODIS) instruments are on board these two satellites, with 36 bands available including 8 thermal infrared bands designed for retrieving of sea surface temperature (SST) and land surface temperature (LST). Two algorithms are used by NASA officially for global surface temperature retrieval from MODIS data (Wan and Dozier, 1996; Wan and Li, 1997), which in total provide four daily global surface temperature coverages. NOAA has two similar meteorological satellites AVHRR with two thermal bands which can accurately retrieve sea surface temperature. Thus people tend to use the SST obtained from AVHRR to supplement ocean surface temperature in previous studies (Hansen et al., 1999; Brohan et al., 2006; Fan and Dool, 2008).

Remote sensing can quickly obtain surface temperature over large area, and it has been standardized to keep consistency and ensure accuracy. MODIS can provide highly accurate estimation of land and sea surface temperatures (Wan et al., 2004; Peter et al., 2006; Wan, 1999), which overcome disadvantages of Combined Land-Surface Air and Sea-Surface Water Temperature Index (Land-Ocean Temperature Index). Therefore the surface temperature obtained from MODIS can help us to accurately determine the surface temperature at different regional scale, which is

an important input parameter for various models (like global climate change and ecology).

2. Methods

The satellite sensors provide frequent global coverages to ensure the consistency of the retrieved surface temperature and overcome disadvantages of Combined Land-Surface Air and Sea-Surface Water Temperature Index (Land-Ocean Temperature Index). The resolution of MODIS thermal bands is 1000 m. The algorithms for retrieving surface temperature from MODIS are mature and NASA has provided the surface temperature product (Wan and Li, 1997; Brown et al., 1999). The surface temperature algorithm and products have been validated in many studies, and there are quality controls for each pixel which has become a standard (Wan et al., 2004; Wan, 2008).

There are seven MODIS LST products, including MOD11_L2, MOD11A1, MOD11B1, MOD11A2, MOD11C1, MOD11C2, and MOD11C3 (Wan, 2008). Different products are generated for different application targets using daily cloudless data. Three products are used in this study. The third product (MOD11B1) is a tile of daily LST and emissivities at 6 km spatial resolution, which is generated by the day/night LST algorithm (Wan, 2008). The fifth product (MOD11C1) is a global daily LST in a geographic projection, which is generated by assembling the MOD11B1 daily tiles together and resampling the SDSs from 6 km resolution to the 0.05° Climate Modeling Grid (CMG). The seventh product (MOD11C3) is monthly CMG LST, which is averaged from temperatures and emissivity values in the MOD11C1 product. MODIS SST has four products, SST at 1-km (Level 2) and 4.6 km, 36 km, and 1° (Level 3) resolutions with an assessment mask. The Level 2 product is generated daily and has a global coverage. It is used to generate the gridded Level 3 products at daily, every 8 days, monthly, and yearly scale in day and night conditions. The values of temperature are interpolated or extrapolated for cloudy grids. An assessment band is provided for each data set, and more description can be inWan et al. (2004) and Wan (2008). We have calculated global surface temperature from MODIS data more consistency to determine which year is the warmest or coldest. Eq. (1) is used to compute mean spatial daily temperature at time t (1:30, 10:30, 13:30, 22:30).

$$T^t_{mj} = \frac{1}{n}\sum_{i=1}^{i=n} TS^t_j \tag{1}$$

where T_{mj} is the mean temperature of pixel j at time t, and i is the day of the year. Eq. (2) is used to compute the global mean surface temperature at time t.

$$T^t_m = \frac{1}{n}\sum_{i=1}^{i=n}\sum_{j=1}^{j=m} S(j)\,TS^t_{ij} \tag{2}$$

where T^t_m is the mean surface temperature at time t, i is the day of the year, j is the pixel index, $S(j)$ is the area weighting obtained from the model of Earth, TS^t_{ij} is the surface temperature in time (1:30, 10:30, 13:30, 22:30) of the day for the same location. On the other hand, there is no data for Aqua satellite in 2001, so we use the mean values to make analysis. Eq. (3) is used to compute mean surface temperature.

$$T_m = \left(T^{1:30}_m + T^{10:30}_m + T^{13:30}_m + T^{22:30}_m\right)/4 \tag{3}$$

where T_m is the mean surface temperature. The daily mean temperature from 2001 to 2012 in various times (1:30, 10:30, 13:30, 22:30) is computed from MODIS surface temperature product, and the results is shown in Table 1.

As shown in Fig. 1, the daily mean temperature in various times (1:30, 10:30, 13:30, 22:30) is stable from 2001 to 2012. Assuming the warmest and coldest time are 14:00 and 4:30 respectively, we calculate the highest and lowest temperature of the day using Eq. (4a) for points a and b, (4b) for points c and d. The daily maximum and minimum mean temperature are 16.852 °C and 12.14 °C respectively.

$$y1 = B + A\sin[\pi/9.5(t-4.5) - \pi/2] \tag{4a}$$

$$y2 = B + A\sin[\pi/14.5(t-14) + \pi/2] \tag{4b}$$

After making some analysis, we found that the whole function of global surface temperature change cannot be precisely described by a sine function. So we use a polynomial function to fit the daily mean temperature, and get the curve in Fig. 2, and two fitted Eq. (5) have been obtained.

$$Ts(t) = 6.63668 * 10^{-4}t^4 - 0.03015t^3 + 0.44158t^2 - 1.9096t + 14.26623 \quad 4.5 \leqslant t \leqslant 14 \tag{5a}$$

$$Ts(t) = -5.70672 * 10^{-4}t^4 + 0.05049t^3 - 1.61704t^2 + 21.79977t - 88.02869 \quad 14 \leqslant t \leqslant 28.5 \tag{5b}$$

Table 1
Annual mean temperature from 2001 to 2012.

Time	Terr (°C)		Aqua (°C)		Mean (°C)
	10:30	22:30	13:30	1:30	
2001	16.111	12.644			14.3775
2002	16.209	12.807	16.81	12.29	14.529
2003	16.051	12.649	16.885	12.3	14.47125
2004	15.993	12.629	16.72	12.175	14.37925
2005	16.159	12.815	16.943	12.373	14.5725
2006	16.062	12.72	16.842	12.305	14.48225
2007	16.119	12.73	16.889	12.276	14.5035
2008	15.945	12.593	16.684	12.135	14.33925
2009	15.934	12.505	16.876	12.331	14.4115
2010	16.114	12.84	16.879	12.419	14.563
2011	16.012	12.738	16.778	12.311	14.45975
2012	16.099	12.775	16.865	12.347	14.5215
Mean (°C)	16.067	12.704	16.834	12.297	14.46752

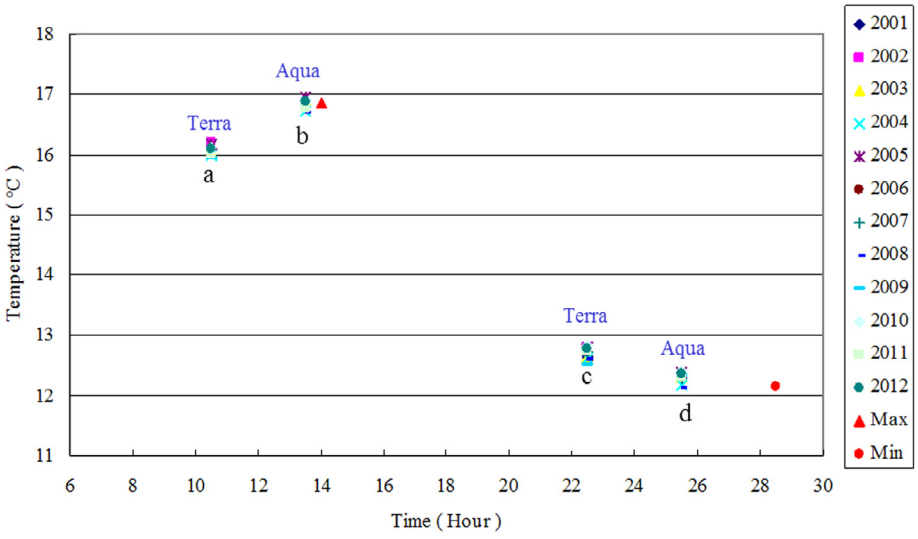

Fig. 1. Daily global mean surface temperature change from 2001 to 2012.

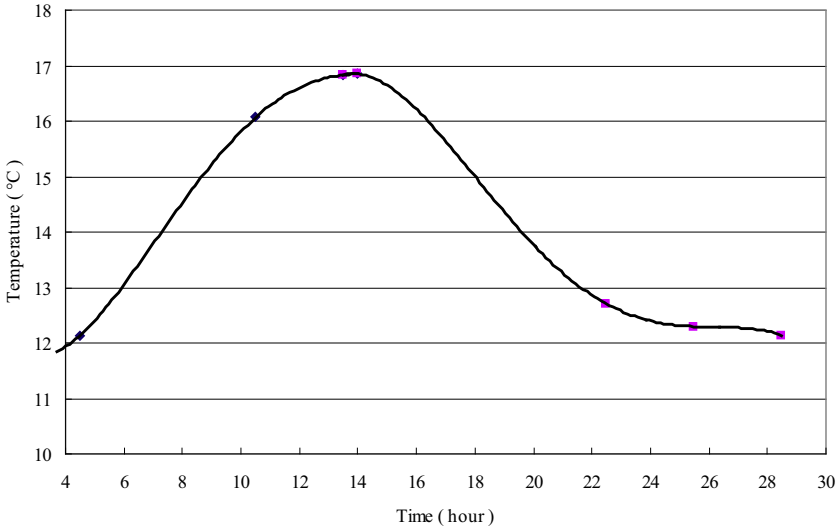

Fig. 2. Change of daily mean temperature in 24 h from 2001 to 2012.

We assume that the times of minimum and maximum temperature are 4:00 and 15:00, and get daily maximum mean temperature (16.9439 °C) and daily minimum mean temperature (12.17356 °C). Two fitted Eq. (6) are obtained.

$$Ts(t) = 6.3819 * 10^{-4}t^4 - 0.02784t^3 + 0.39481t^2 - 1.60976t + 13.91403 \quad 4 \leqslant t \leqslant 15 \tag{6a}$$

$$Ts(t) = -7.76798 * 10^{-4}t^4 + 0.06875t^3 - 2.21206t^2 + 30.21413t - 131.25201 \quad 15 \leqslant t \leqslant 28 \tag{6b}$$

Eq. (5) or (6) can be used to obtain hourly mean temperature in a day. Eq. (7) is used to compute the absolute daily mean surface temperature (T_{am}).

$$T_{am} = Ts(5.5) + Ts(6.5) + \cdots + Ts(28.5)/24 \tag{7}$$

Table 2 is the hourly mean temperature. Comparing the daily mean temperature in Table 2 with Table 1, we found the difference of mean temperature is between 0.04 °C and 0.17 °C, and can conclude that the global mean temperature can be approximately calculated by Eq. (3). Since the observation time is symmetrical, the global mean surface temperature is more approximate to absolute mean surface temperature because of the high coverage of satellite data. The daily mean surface temperatures are calculated by Eq. (3) for ocean, land and globe, 2 hemispheres, 7 continents, and 4 oceans.

3. Results

Gridded surface temperature can be obtained in various times (1:30, 10:30, 13:30, 22:30) during the day. Fig. 3 is spatial distribution of daily mean temperature in various

Table 2
Fitted daily mean temperature calculated by Eqs. (5) and (6).

Daily time (h)	Eq. (5) (°C)	Eq. (6) (°C)
5.5	12.71232	12.95546
6.5	13.41533	13.62496
7.5	14.16346	14.32317
8.5	14.8873	14.99024
9.5	15.53339	15.58169
10.5	16.06416	16.06831
11.5	16.458	16.43624
12.5	16.70922	16.6869
13.5	16.82805	16.83707
14.5	16.84067	16.91882
15.5	16.45311	16.79917
16.5	15.93752	16.30508
17.5	15.32084	15.65377
18.5	14.67316	14.9408
19.5	14.0509	14.24309
20.5	13.49678	13.61894
21.5	13.0398	13.10797
22.5	12.6953	12.73118
23.5	12.46489	12.49091
24.5	12.33651	12.37089
25.5	12.28438	12.33616
26.5	12.26906	12.33315
27.5	12.23736	12.28965
28.5	12.12245	12.11477
Mean (°C)	14.29141	14.4066

times (1:30, 10:30, 13:30, 22:30) in 2012, which shows the difference of global surface temperature in different times. Shown from Fig. 3, the change in temperature at different times of the day is mainly caused by the Earth's rotation. For example, the diurnal temperature difference is very large in Africa and Australia.

Since the observation time is symmetrical, the global mean surface temperature approximates to absolute mean surface temperature because of the frequent coverage of satellite data. Terra and Aqua satellites are launched by NASA in 1999 and 2002 respectively. Fig. 4 shows the spatial distribution of global mean surface temperature from 2001 to 2012, indicating that the highest temperature is located between 50°N and 50°N, and the lowest temperature is in Antarctica.

NASA-GISS, HadCRUT3, NOAA-NCDC and Japan Meteorological Agency (JMA) made four independent analyses with periods of records extending back to the mid-to-late 1800s (Hansen et al., 2010; Brohan et al., 2006; Smith et al., 2008; Ishihara, 2006), and the warmest year cannot be certainly determined. According to NOAA scientists, 2010 tied with 2005 are the warmest years in the global surface temperature record since 1880 (NOAA, 2010), while the United Kingdom archive places 2005 second behind 1998 (Shein et al., 2006). Two main reasons may be responsible for inconsistency. One is that the observation sites are inadequate and unevenly distributed, and the other is that the Sea-Surface Water Temperature Index (Land-Ocean Temperature Index) is obtained from NOAA/AVHRR, which provides SST twice a day (Hansen et al., 1999). Although the diurnal difference in mean sea surface temperature is within 1 °C, this difference is sufficient to cause such uncertainty. MODIS data can provide surface temperature four times a day, allowing better estimation of the daily temperature, which is reliable to determine the warmest and coldest years globally and region. Therefore, we computed the annual mean temperature for ocean, land, and the globe from 2001 to 2012, which is shown in Table 3. The global mean surface temperature is 14.46 °C computed from MODIS data (Table 1). We proposed a method to calculate mean surface temperature based on remote sensing data and global absolute mean temperature is close to 14.35 °C (the mean in Table 2) in recent twelve years, and the warmest and coldest years for the globe are 2005 and 2008, respectively. The mean land surface temperature in 2005 is higher than in 2010, but the mean sea surface temperature is almost equal in 2005 and 2010. The coldest year is 2008 without controversy because of the lowest sea surface temperature in the past twelve years. Although the mean land surface temperature in not very low, the ocean, however, accounts for 71% of the Earth's surface, therefore 2008 is the lowest year due to the La Niña (Peterson and Baringer, 2009). The mean surface temperature of land is 8.75 °C, and the warmest and coldest years are 2005 and 2001, respectively. The mean surface temperature of ocean is 16.79 °C, and the warmest and coldest years are 2010 and 2008, respectively. Table 3 shows that the global warming trend is weak and insignificant in recent twelve years.

The surface temperature is also different in the two hemispheres (Table 3). The mean surface temperature of the Northern Hemisphere is 15.69 °C, and the warmest and coldest years are 2002 and 2001, respectively. The mean surface temperature of the Southern Hemisphere is 13.25 °C, and the warmest and coldest years are 2005 and 2002, respectively. Higher temperature in the Southern Hemisphere in 2005 has greatly contributed to the high global mean temperature. In the past twelve years, the Southern Hemisphere is warming ($P = 0.0129$ °C/year), while the Northern Hemisphere is slightly cooling ($P = -0.0053$ °C/year).

The mean surface temperatures of seven continents are also different (Table 3). The mean surface temperature of North America is 1.93 °C, and the warmest and coldest years are 2010 and 2008, respectively. The mean surface temperature of South America is 21.2 °C, and the warmest and coldest years are 2002 and 2001, respectively. The mean surface temperature of Asia in the recent 12 years is 8.79 °C, and the warmest and coldest years are 2007 and 2002. The mean surface temperature of Europe is 4.9 °C, and the warmest and coldest years are 2007 and 2002. The mean surface temperature of Oceania is 24.41 °C, and the warmest and coldest years are 2002 and 2001, respectively. The mean surface temperature of Africa is 25.18 °C, and the warmest and coldest years are 2010 and 2001, respectively. The mean surface temperature of Antarctic is −40.5 °C, and the warmest and coldest years are 2002 and 2001, respectively. Among the seven conti-

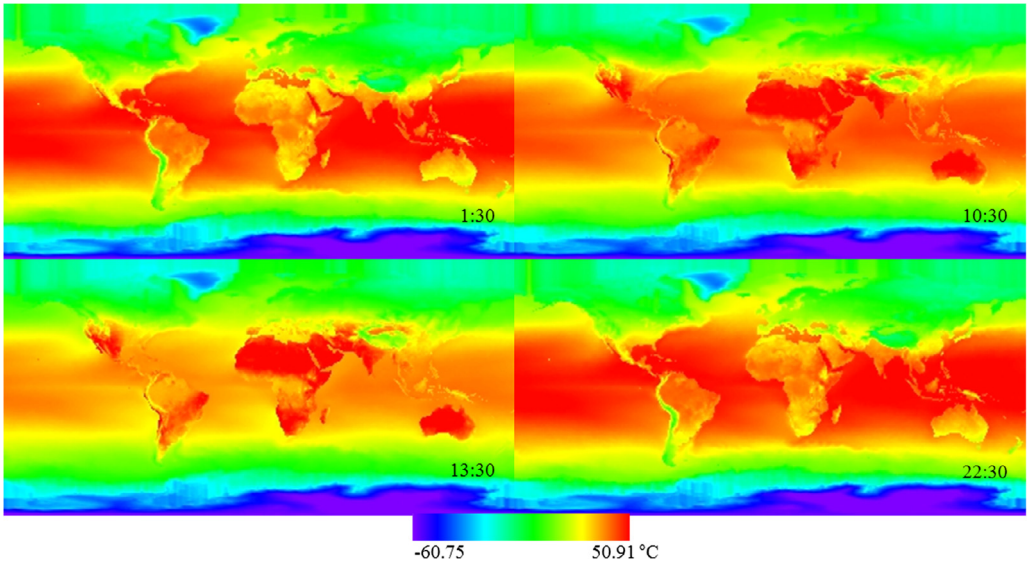

Fig. 3. Daily mean temperature (°C) in various times (1:30, 10:30, 13:30, 22:30) in 2012.

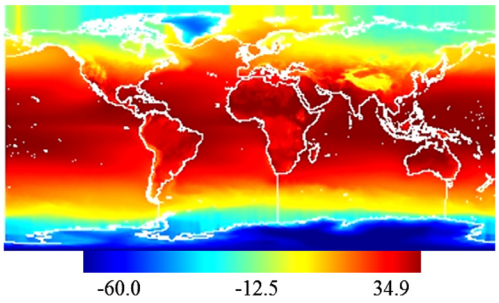

Fig. 4. The mean surface temperature (°C) from 2001 to 2012.

nents, only Oceania is cooling in the recent twelve years ($P = -0.0685$ °C/year).

The surface temperatures of the four oceans are very different from the continents (Table 3). The mean surface temperature of Pacific Ocean is 18.96 °C, and the warmest and coldest years are 2002 and 2008. The mean surface temperature of Atlantic Ocean is 16.39 °C, and the warmest and coldest years are 2010 and 2002. The mean surface temperature of Indian Ocean is 17.34 °C, and the warmest and coldest years are 2010 and 2002. The mean surface temperature of Arctic Ocean is −7.18 °C, and the warmest and coldest years are 2002 and 2004, respectively. In recent twelve years, Indian Ocean is warming ($P = 0.0285$ °C/year), while the Pacific Ocean is cooling ($P = -0.0182$ °C/year).

In order to get the global change rate of surface temperature in detail, a linear regression has been conducted using every pixel from 2001 to 2012, and the slope is used to represent the change rate of the surface temperature (Fig. 5a). Fig. 5b is the distribution map of correlation coefficient, and the correlation coefficient is also very high in the place

Table 3
Mean temperature for ocean, land and globe, 2 hemispheres, 7 continents, and 4 oceans.

Globe and regions	Yearly mean temperature (°C)											2012
	2001	2002	2003	2004	2005	2006	2007	2008	2009	2010	2011	
Globe	14.377	14.529	14.471	14.379	14.572	14.482	14.504	14.339	14.411	14.563	14.46	14.522
Land	8.391	8.953	8.784	8.583	8.964	8.705	8.947	8.635	8.716	8.874	8.682	8.79
Ocean	16.814	16.799	16.786	16.738	16.855	16.833	16.765	16.661	16.729	16.878	16.812	16.854
Northern Hemisphere	15.539	15.996	15.694	15.555	15.79	15.724	15.733	15.542	15.546	15.826	15.615	15.699
Southern Hemisphere	13.215	13.063	13.249	13.203	13.355	13.24	13.274	13.137	13.276	13.3	13.305	13.344
North America	1.952	2.131	2.037	1.265	2.131	2.476	1.589	1.222	1.425	2.695	1.641	2.541
South American	20.721	21.728	21.259	21.095	21.253	21.069	21.151	21.091	21.177	21.458	21.006	21.426
Asia	8.668	8.604	8.759	8.796	8.934	8.694	9.321	8.945	8.643	8.775	8.772	8.619
Europe	4.427	4.219	4.898	4.677	5.166	4.753	5.763	5.503	4.791	4.424	5.333	4.902
Oceania	23.061	25.79	24.834	24.478	25.256	24.414	24.741	24.433	24.865	23.757	23.153	24.142
Africa	24.718	25.274	25.275	25.119	25.356	24.996	25.142	25.055	25.335	25.663	25.167	25.112
Antarctic	−41.296	−39.182	−40.767	−40.767	−40.144	−40.993	−40.164	−41.066	−39.95	−41.162	−39.92	−40.583
Pacific Ocean	18.981	19.147	19.016	19.035	19.065	19.022	18.866	18.798	18.918	18.847	18.855	18.994
Atlantic Ocean	16.413	16.193	16.359	16.317	16.473	16.519	16.309	16.323	16.236	16.666	16.47	16.344
Indian Ocean	17.466	16.958	17.309	17.265	17.222	17.181	17.446	17.265	17.399	17.545	17.509	17.507
Arctic Ocean	−7.678	−6.266	−7.666	−8.482	−6.905	−6.987	−6.839	−7.632	−7.575	−6.562	−6.861	−6.738

where the temperature changes greatly. The central and eastern regions of Pacific Ocean, northern regions of Atlantic Ocean, northern regions of China, Mongolia, southern regions of Russia, western regions of Canada and America, the eastern and northern regions of Australia, and the southern tip of Africa are cooling, and most of the other regions are warming in the recent twelve years.

We further analyzed the seasonal variations of the surface temperature from 2001 to 2012, and the results are given in Fig. 6. It is interesting to find that the surface temperature changes significantly from the spring season (March–May) to the winter season (December–February) in the northern hemisphere. Especially in winter, temperature changes are particularly evident in the northern hemisphere. On the contrary, the inter-seasonal surface temperature change is not obvious in the southern hemisphere. The seasonal variations of surface temperature are mainly affected by the Earth's revolution.

The change trends of the global surface temperature by seasons are given in Fig. 7, and Fig. 8 is the distribution map of correlation coefficient by seasons from 2001 to 2012. There is a yearly decreasing trend in the north-east part of North America and Eastern Australia, and a yearly increasing trend in north-west of North America and North Asia. It is decreasing obviously in Greenland in the spring and autumn, while it is increasing in Greenland in summer and winter. In Antarctica, the surface temperature is decreasing in the spring, while it is increasing in the summer and autumn. Mao et al. (2016a,b) analyzed the change of global water vapor and vegetation, and found that vegetation, water vapor content and surface temperature increased simultaneously in the northern high latitude regions. The increase of atmospheric water vapor and temperature increase is the main reasons for the increase of vegetation, especially in winter and spring (shown in Figs. 7 and 8). The global carbon dioxide is increasing, while the global temperature is fluctuating in recent years. There are two main reasons. The one is that the global vegetation change is the bridge among the temperature and water vapor content and carbon dioxide (CO_2), and global

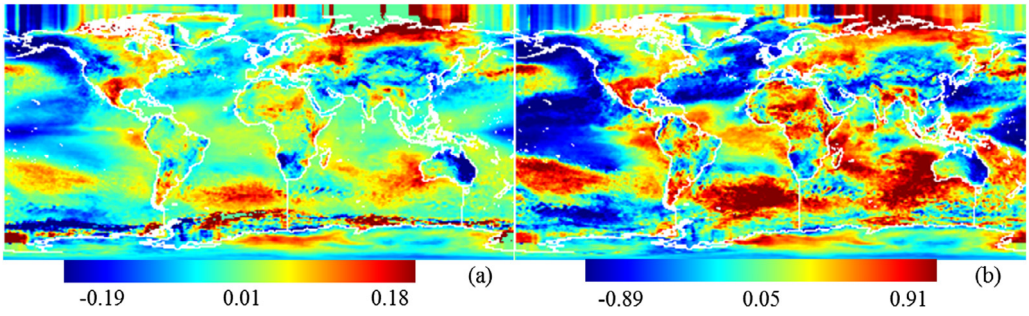

Fig. 5. Global surface temperature change from 2001 to 2012: (a) rate (slope) of linear regression and (b) correlation coefficient.

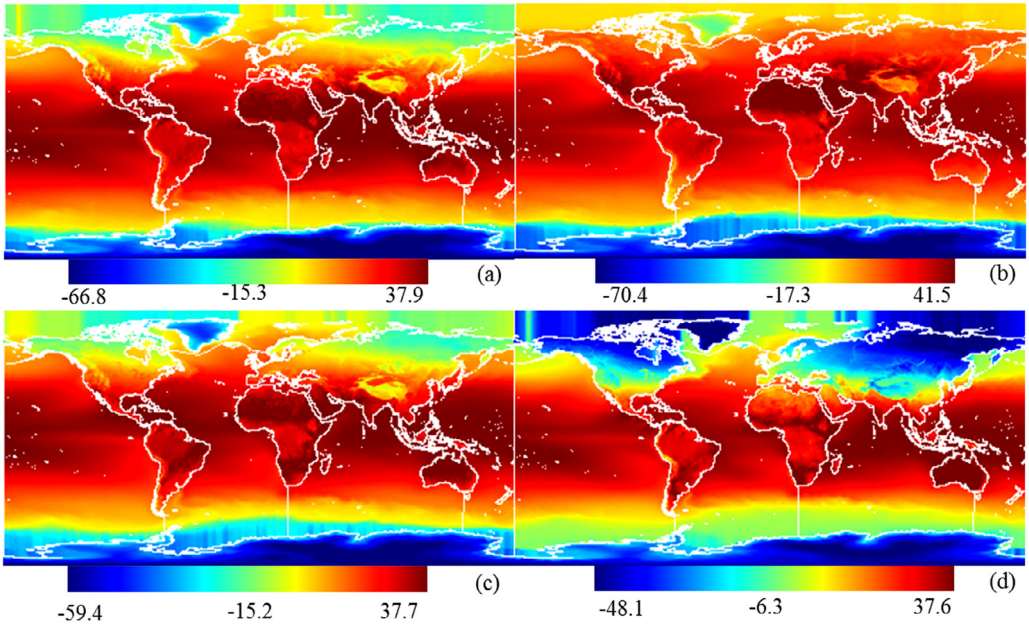

Fig. 6. The change of mean surface temperature (°C) by seasons from 2001 to 2012: (a) March–May; (b) June–August; (c) September–November; and (d) December–February.

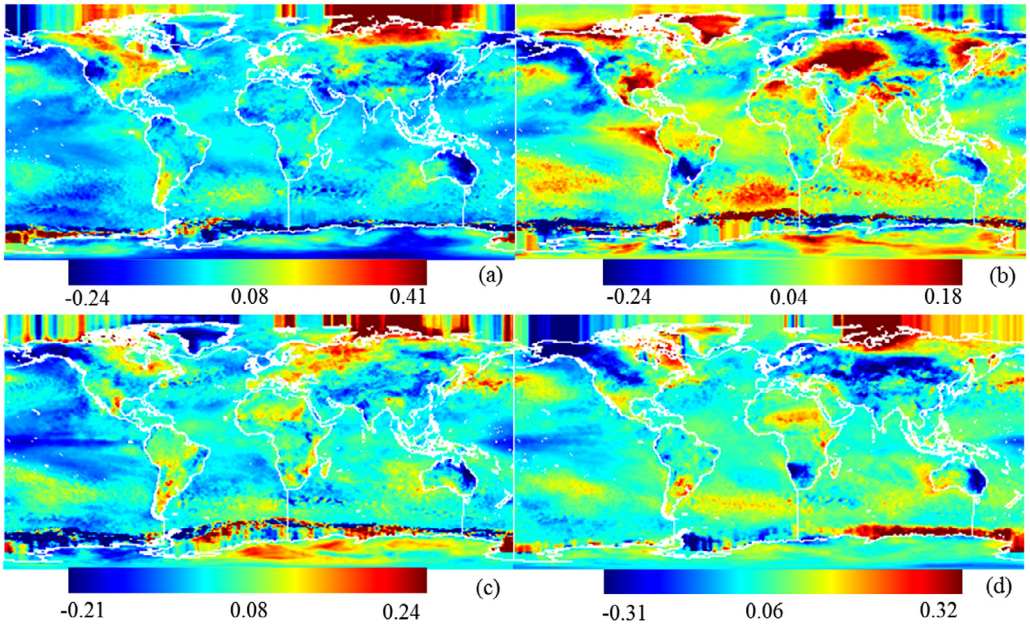

Fig. 7. The overall change rate of the surface temperature by seasons from 2001 to 2012: (a) March–May; (b) June–August; (c) September–November; and (d) December–February.

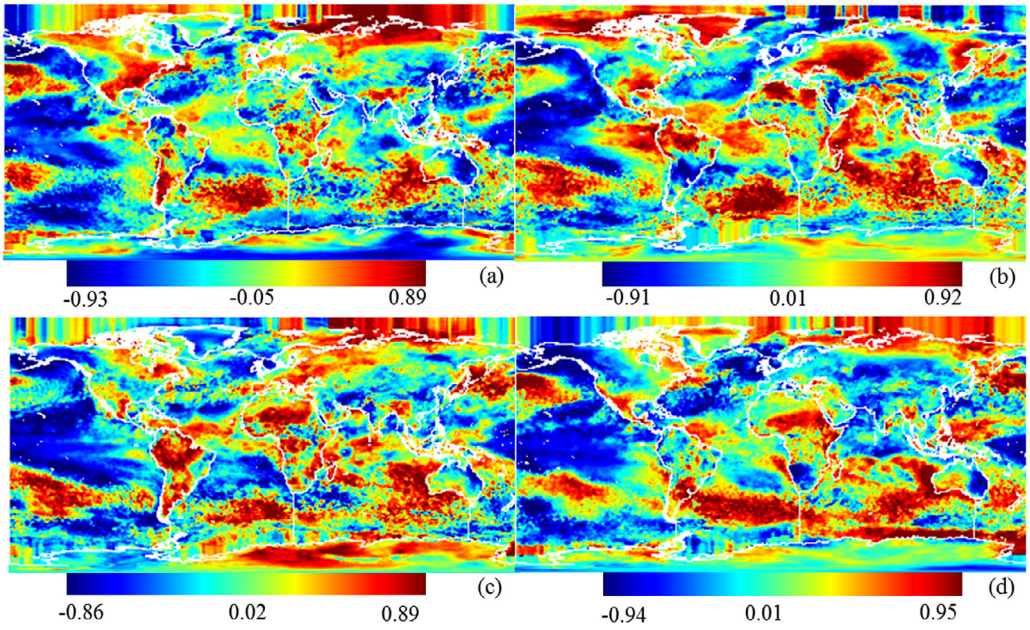

Fig. 8. The distribution map of correlation coefficient by seasons from 2001 to 2012: (a) March–May; (b) June–August; (c) September–November; and (d) December–February.

vegetation through the water vapor and carbon dioxide to regulate the global temperature change, and the other reason is that the global water vapor content is decreasing (Mao et al., 2016a,b). Earth's daily temperature change is determined by the Earth's rotation, and the Earth's temperature change from spring to winter is due to the Earth revolution around the Sun. The Earth's inter-annual temperature change is determined by the revolution of the other stars inside the solar system, and the longer period of temperature change is determined by the revolution of the solar system. In a word, the temperature change is mainly determined by the variation of orbit of celestial body, and carbon dioxide has little effect on global temperature changes. We proposed to build a big data model based on orbit position and gravitational-magmatic change of celestial body with the solar or the galactic system, and the principal of this model is that the climate and ecosystem changes such as temperature and water cycle are

mainly determined by the Earth's orbit position in the solar and galaxy system which indirectly affects the temporal and spatial variation of vegetation at large scale (Mao et al., 2015, 2016a,b). There might be more contributing factors to affect the temperature, which requires further attention.

4. Discussion and conclusion

Global climate change is in the hot topic. Surface temperature change is one of the most important aspects. Previous research primarily relies on ground observations, but limited by the available of observation sites. For security reasons, stations in most countries just provide mean, maximum, and minimum temperature causing large uncertainty. Satellite remote sensing can overcome these shortcomings and ensure the consistency of measurement. Therefore, it is very important to use remote sensing technology for obtaining surface temperature over large area. This method based on remote sensing technique will greatly impact climate change research and even for the satellite design. There are also three shortcomings of satellite remote sensing technology. One is that satellites have life cycle, and the number of measurements for globe per day is not enough. The other is that the accuracy of some sensors needs to be further improved. AVHRR/NOAA are not suitable very well to be used to do this work because it cannot retrieve accurately land surface temperature, and the thermal sensors at satellite should be designed like MODIS in Terra and Aqua.

This study uses the surface temperature obtained from remote sensing data, and a new method is proposed to calculate the mean surface temperature. The global mean surface temperature is 14.35 °C from 2001 to 2012, and the warmest and coldest surface temperatures of the global in recent twelve years occurred in 2005 and 2008. The warmest and coldest surface temperatures on the global land surface occurred in 2005 and 2001, and on the global ocean surface in 2010 and 2008. Temperatures for the two hemispheres, the seven continents, and the four Oceans are also obtained. In the recent twelve years, the global warming trend is weak and insignificant, and the surface temperature in Northern hemisphere is decreasing slightly, while is increasing slightly in Southern Hemisphere.

The seasonal variations of surface temperature indicated that there is a year-round decreasing trend in the north-east part of North America and Eastern Australia, while a yearly increasing trend is found in north-west of North America and North Asia. It is decreasing clearly in Greenland in the spring and autumn, while it is increasing in Greenland in summer and winter. In Antarctica, the surface temperature is decreasing in the spring, while it is increasing in the summer and autumn. The change in temperature at different times per day is determined by the Earth's rotation, and the seasonal variations of surface temperature are mainly determined by the Earth's revolution. The Earth's inter-annual temperature changes are determined by the revolution of the stars in the solar system, and the longer period of temperature change is determined by the revolution of the solar system. A big data model should be built based on orbit position and gravitational-magmatic change of celestial body with the solar or the galactic system.

Acknowledgements

The Authors would like to thank the Goddard Space Flight Center for providing the MODIS data, and Dr. Tony from the University of Toronto for improving the English. This work was supported by National Natural Science Foundation of China (No. 41571427), the National Key Project of China (No. 2016YFC0500203), and Open Fund of State Key Laboratory of Remote Sensing Science (Grant No. OFSLRSS 201515).

References

Becker, F., Li, Z.L., 1990. Towards a local split window method over land surfaces. Int. J. Remote Sens. 11, 369–393.

Brohan, P., Kennedy, J.J., Harris, I., Tett, S.F.B., Jones, P.D., 2006. Uncertainty estimates in regional and global observed temperature changes: a new data set from 1850. J. Geophys. Res. 111 (D12106), 1–21. http://dx.doi.org/10.1029/2005JD006548.

Brown, Otis B., Minnett, Peter J., with Contributions from: Evans, R., Kearns, E., Kilpatrick, K., Kumar, A., Sikorski, R., Závody, A., 1999. MODIS Infrared Sea Surface Temperature Algorithm Theoretical Basis Document (SST ATBD) Version 2, University of Miami, Miami, FL 33149–1098.

Fan, Y., Dool, H.V.D., 2008. A global monthly land surface air temperature analysis for 1948 – present. J. Geophys. Res. 113 (D01103), 1–18. http://dx.doi.org/10.1029/2007JD008470.

Gillespie, A.R., Rokugawa, S., Matsunaga, T., Cothern, J.S., Hook, S., Kahle, A.B., 1998. A temperature and emissivity separation algorithm for Advanced Spaceborne Thermal Emission and Reflection Radiometer (ASTER) images. IEEE Trans. Geosci. Remote Sens. 36, 1113–1126.

Hansen, J.E., Lebedeff, S., 1987. Global trends of measured surface air temperature. J. Geophys. Res. 92, 13345–13372. http://dx.doi.org/10.1029/JD092iD11p13345.

Hansen, J., Fung, I., Lacis, A., Rind, D., Ruedy, L.R., Russell, G., Stone, P., 1988. Global climate changes as forecast by Goddard Institute for space studies three-dimensional model. J. Geophys. Res. 93 (D8), 9341–9364.

Hansen, J., Ruedy, R., Glascoe, J., Sato, M., 1999. GISS analysis of surface temperature change. J. Geophys. Res. 104, 30997–31022. http://dx.doi.org/10.1029/1999JD900835.

Hansen, J., Ruedy, R., Sato, M., Imhoff, M., Lawrence, W., Easterling, D., Peterson, T., Karl, T., 2001. A closer look at United States and global surface temperature change. J. Geophys. Res. 106, 23947–23963. http://dx.doi.org/10.1029/2001JD000354.

Hansen, J., Sato, M., Ruedy, R., Lo, K., Lea, D.W., Medina-Elizade, M., 2006. Global temperature change. Proc. Natl. Acad. Sci. 103, 14288–14293. http://dx.doi.org/10.1073/pnas.0606291103.

Hansen, J., Ruedy, R., Sato, M., Lo, K., 2010. Global surface temperature change. Rev. Geophys. 48, RG4004. http://dx.doi.org/10.1029/2010RG000345.

Hansen, J., Sato, M., Ruedy, R., 2012. Perception of climate change. PNAS 6, 2415–2423. http://dx.doi.org/10.1073/pnas.1205276109.

Hook, S.J., Gabell, A.R., Green, A.A., Kealy, P.S., 1992. A comparison of techniques for extracting emissivity information from thermal infrared data for geologic studies. Remote Sens. Environ. 42, 123–135.

Ishihara, K., 2006. Calculation of global surface temperature anomalies with COBE-SST. Sokko-jiho. Weather Serv. Bull. 73 (Special Issue), S19–S25 (in Japanese).

Jiménez-Muñoz, J.C., Sobrino, J.A., 2003. A generalized single-channel method for retrieving land surface temperature from remote sensing data. J. Geophys. Res. 108, 4688–4695.

Jones, P.D., New, M., Parker, D.E., Martin, S., Rigor, I.G., 1999. Surface air temperature and its changes over the past 150 years. Rev. Geophys. 37, 173–199.

Kealy, P.S., Hook, S.J., 1993. Separating temperature and emissivity in thermal infrared multispectral scanner data: Implications for recovering land surface temperatures. IEEE Trans. Geosci. Remote Sens. 31, 1155–1164.

Kerr, Y.H., Lagouarde, J.P., Imbernon, J., 1992. Accurate land surface temperature retrieval from AVHRR data with use of an improved split window algorithm. Remote Sens. Environ. 41, 197–209.

Li, Z.L., Wu, H., Wang, N., Qiu, S., Sobrino, J.A., Wan, Z., Tang, B.H., Yan, G.J., 2013a. Review article: Land surface emissivity retrieval from satellite data. Int. J. Remote Sens. 34, 3084–3127.

Li, Z.L., Tang, B.H., Wu, H., Ren, H.Z., Yan, G.J., Wan, Z.M., Trigo, I. F., Sobrino, J.A., 2013b. Satellite-derived land surface temperature: current status and perspectives. Remote Sens. Environ. 131, 14–37.

Mao, K.B., Qin, Z., Shi, J., Gong, P., 2005. A practical split-window algorithm for retrieving land surface temperature from MODIS data. Int. J. Remote Sens. 26, 3181–3204.

Mao, K.B., Shi, J., Li, Z.L., Tang, H., 2007. An RM-NN algorithm for retrieving land surface temperature and emissivity from EOS/MODIS data. J. Geophys. Res. 112 (D21102), 1–17.

Mao, K.B., Ma, Y., Xu, T.R., Liu, Q., Han, J.Q., Xia, L., Shen, X.Y., He, T.J., 2015. A new perspective about climate change. Sci. J. Earth Sci. 5 (1), 12–17.

Mao, K.B., Ma, Y., Zuo, Z.Y., Jiao, Y.Q., Wang, F., Liu, Q., Sun, Z.W., 2016a. Global water vapor content and vegetation change analysis based on remote sensing data. International Geoscience and Remote Sensing Symposium, vol. 16, pp. 5205–5208.

Mao, K.B., Ma, Y., Zuo, Z.Y., Wang, F., Jiao, Y.Q., Shen, X.Y., Liu, Q., 2016b. Which year is the hottest or coldest from 2001-2012 based on remote sensing data. International Geoscience and Remote Sensing Symposium, vol. 16, pp. 5213–5216.

McMillin, L.M., 1975. Estimation of sea surface temperature from two infrared window measurements with different absorptions. J. Geophys. Res. 80, 5113–5117.

NOAA: 2010 Tied For Warmest Year on Record. <http://www.noaanews.noaa.gov/stories2011/20110112_globalstats.html>.

Peter, J., Minnett, R. H., Evans with Kay, K., Ajoy, K., Warner, B., 2006. Validation of Sea-Surface Temperatures from MODIS. MODIS Science Team Meeting, MCST Session, Nov. 1, pp. 1–29.

Peterson, T.C., Baringer, M.O. (Eds.), 2009. State of the Climate in 2008, Bull. Am. Meteorol. Soc., vol. 90, pp. S1–S196.

Pozo, V.D., Olmo Reyes, F.J., Alados, A.L., 1997. A comparative study of algorithms for estimating land surface temperature from AVHRR data. Remote Sens. Environ. 62, 215–222.

Price, J.C., 1983. Estimating surface temperatures from satellite thermal infrared data: a simple formulation for the atmospheric effect. Remote Sens. Environ. 13, 353–361.

Price, J.C., 1984. Land surface temperature measurements from the split window channels of the NOAA 7 AVHRR. J. Geophys. Res. 89, 7231–7237.

Qin, Z., Karnieli, A., Berliner, P., 2001. A mono-window algorithm for retrieving land surface temperature from Landsat TM data and its application to the Israel-Egypt border region. Int. J. Remote Sens. 22, 3719–3746.

Rahmstorf, S., Coumou, D., 2011. Increase of extreme events in a warming world. Proc. Natl. Acad. Sci. U.S.A. 108, 17905–17909.

Rayner, N.A., Parker, D.E., Horton, E.B., Folland, C.K., Alexander, L. V., Rowell, D.P., Kent, E.C., Kaplan, A., 2003. Global analyses of sea surface temperature, sea ice, and night marine air temperature since the late nineteenth century. J. Geophys. Res. 108 (D14), 1–22. http://dx.doi.org/10.1029/2002JD002670, 4407.

Reynolds, R.W., Zhang, H.M., Smith, T.M., Gentemann, C.L., Wentz, F., 2005. Impacts of in situ and additional satellite data on the accuracy of a sea-surface temperature analysis for climate. Int. J. Climatol. 25, 857–864.

Shein, K.A., Contributing Ed., Eds., 2006: State of the Climate in 2005. Bull. Am. Meteorol. Soc., vol. 87, pp. 1–104.

Smith, T.M., Reynolds, R.W., Peterson, T.C., Lawrimore, J., 2008. Improvements to NOAA's historical merged land-ocean surface temperature analysis (1880–2006). J. Clim. 21, 2283–2296.

Susskind, J., Rosenfield, J., Reuter, D., Chahine, M.T., 1984. Remote sensing of weather and climate parameters from HIRS2/MSU on TIROS-N. J. Geophys. Res. 89, 4677–4697.

Wan, Z.M., 1999. MODIS Land-Surface Temperature Algorithm Theoretical Basis Document (LST ATBD). Version 3.3. Institute for Computational Earth System Science, University of California, Santa Barbara, CA.

Wan, Z., 2008. New refinements and validation of the MODIS land-surface temperature/emissivity products. Remote Sens. Environ. 112, 59–74.

Wan, Z., Dozier, J., 1996. A generalized split-window algorithm for retrieving land-surface temperature from space. IEEE Trans. Geosci. Remote Sens. 34, 892–905.

Wan, Z., Li, Z.L., 1997. A physics-based algorithm for retrieving land-surface emissivity and temperature from EOS/MODIS data. IEEE Trans. Geosci. Remote Sens. 35 (4), 980–996.

Wan, Z., Zhang, Y., Zhang, Q., Li, Z.L., 2004. Quality assessment and validation of the MODIS global land surface temperature. Int. J. Remote Sens. 25, 261–274.